articles

molecular pharmaceutics

Controlled Nitric Oxide Delivery Platform Based on *S*-Nitrosothiol Conjugated Interpolymer Complexes for Diabetic Wound Healing

Yan Li and Ping I. Lee*

Department of Pharmaceutical Sciences, Leslie Dan Faculty of Pharmacy, University of Toronto, Toronto, Ontario M5S 3M2, Canada

Received September 20, 2009; Revised Manuscript Received December 7, 2009; Accepted December 23, 2009

Abstract: Nitric oxide (NO) is known to play a critical role in enhancing wound healing as topical NO administration has demonstrated enhanced wound healing in diabetic animal models. However, this approach has been limited by the short duration of NO release, short half-life of NO, and instability of available NO donors. To overcome these deficiencies, we have developed a new NO delivery platform based on grafting *S*-nitrosothiols (RSNOs), derived from endogenous glutathione (GSH) or its oligomeric derivatives, phytochelatins (PCs), onto poly(vinyl methyl ether-*co*-maleic anhydride) (PVMMA), and their subsequent formation of interpolymer complexes with poly(vinyl pyrrolidone) (PVP). Such interpolymer complexes provide controlled release of NO for an extended duration (>10 days) and exhibit enhanced stability in the solid state over that of free RSNOs. The existence of intermolecular hydrogen bonding in such complexes and the formation of disulfide bonds following the NO release have been confirmed by FTIR and Raman. Preliminary wound healing study in a diabetic rat model demonstrates that, with a single topical application, the present controlled release NO delivery system can effectively accelerate wound closure as compared with the control ($p < 0.05$). The results suggest that the present NO releasing interpolymer complexes could be potentially useful for diabetic wound healing.

Keywords: Nitric oxide; controlled release; interpolymer complex; *S*-nitrosothiols; diabetic wound healing

Introduction

Nitric oxide (NO) is a ubiquitous biological mediator converted endogenously from L-arginine by nitric oxide synthases (NOS). The key physiological roles of NO in cardiovascular, nervous and immune systems have been identified and elucidated in recent years.[1−3] As a result, a number of potential therapeutic applications of exogenous NO delivery in cardiovascular diseases, respiratory diseases, cancer treatment, antimicrobial therapy, wound healing, and functional biomedical devices have been proposed and explored.[4−8] Among the numerous benefits of NO, its critical

* To whom correspondence should be addressed. Mailing address: Leslie Dan Faculty of Pharmacy, University of Toronto, 144 College Street, Toronto, Ontario M5S 3M2, Canada. Tel: +1-416-946-0606. Fax: +1-416-978-8511. E-mail: ping.lee@utoronto.ca.

(1) Barbato, J. E.; Tzeng, E. Nitric oxide and arterial disease. *J. Vasc. Surg.* **2004**, *40*, 187–193.

(2) Toda, N.; Okamura, T. The pharmacology of nitric oxide in the peripheral nervous system of blood vessels. *Pharmacol. Rev.* **2003**, *55*, 271–324.

(3) Taylor, E. L.; Megson, I. L.; Haslett, C.; Rossi, A. G. Nitric oxide: a key regulator of myeloid inflammatory cell apoptosis. *Cell Death Differ.* **2003**, *10*, 418–430.

(4) Groves, P. H.; Banning, A. P.; Penny, W. J.; Newby, A. C. The effects of exogenous nitric-oxide on smooth-muscle cell-proliferation following porcine carotid angioplasty. *Cardiovasc. Res.* **1995**, *30*, 87–96.

(5) Ricciardolo, F. L. M.; Sterk, P. J.; Gaston, B.; Folkerts, G. Nitric oxide in health and disease of the respiratory system. *Physiol. Rev.* **2004**, *84*, 731–765.

(6) Wei, D. Y.; Richardson, E. L.; Zhu, K. Y.; Wang, L. W.; Le, X. D.; He, Y. J.; Huang, S. Y.; Xie, K. P. Direct demonstration of negative regulation of tumor growth and metastasis by host-inducible nitric oxide synthase. *Cancer Res.* **2003**, *63*, 3855–3859.

10.1021/mp900237f
Published on Web 12/23/2009

role in the overall wound healing process involving granulation tissue formation, epidermal migration, collagen deposition and angiogenesis has motivated the pursuit of topical administration of NO and NO donors in promoting the healing of diabetic ulcers where impaired wound healing has been linked to NO and NOS deficiencies at the wound site.[9−11] Such localized and topical delivery of NO is particularly advantageous as NO is only targeted to the specific wound site without eliciting a systemic load. However, these modes of treatment have been limited by the short duration of NO release, short half-life of NO in the physiological fluid, and instability of available NO donors.[9,12,13]

A range of NO donors derived from two major families of NO precursors such as diazeniumdiolates (NONOates) and *S*-nitrosothiols have been studied extensively.[14−16] In an attempt to prolong the NO release for localized and topical delivery, NONOates have been incorporated into hydrophobic polymers such as polyurethane and poly(vinyl chloride) to provide extended NO release for a duration of from several hours up to a week.[17−19] However, the clinical utility of NONOates has been limited by the potential toxicity of the parent compound and byproduct of NONOate metabolism, particularly the possibility of forming carcinogenic secondary nitrosamines.[20,21] Although C-based NONOates have been proposed to avoid the formation of carcinogenic nitrosoamines,[22] not all such NONOates can release NO spontaneously,[23] nor can they be readily adaptable to wound healing applications.[24]

On the other hand, *S*-nitrosothiols (with generic structure, RSNO) represent an important and a more desirable class of NO donors because they occur endogenously as *S*-nitrosoglutathione (GSNO) or as RSNOs of sulfur-containing peptides and proteins.[15,25] However, the stability of these RSNOs is often less than desirable as the S−NO bond is both thermally and photolytically labile, and susceptible to homolytic cleavage catalyzed by metal ions leading to the rapid release of NO with the corresponding formation of disulfides,[26] thus limiting their suitability for localized and topical delivery of NO. In order to improve the stability and prolong the effective duration of RSNOs, a number of approaches have been pursued. One strategy involves the modification of molecular structure of low-molecular weight RSNOs to increase their lipophilicity,[27] or to impart pH-controlled NO release properties.[28] These synthetic RSNOs and their decomposition products often involve chemical moieties of unknown pharmacological and toxicological nature thereby limiting their acceptability for in vivo applications. Another approach involves conjugating NO to larger peptides and proteins such as bovine serum albumin (BSA) or PEG-conjugated BSA through the cysteine residues.[29,30] In addition to rapid NO release, another major drawback of these NO donors is their low level of achievable NO loading due to the limited cysteine content of BSA.

(7) Ghavari, A.; Miller, C. C.; McMullin, B.; Ghahary, A. Potential application of gaseous nitric oxide as a topical antimicrobial agent. *Nitric Oxide* **2006**, *14*, 21–29.

(8) Witte, M. B.; Barbul, A. Role of nitric oxide in wound repair. *Am. J. Surg.* **2002**, *183*, 406–412.

(9) Isenberg, J. S.; Ridnour, L. A.; Espey, M. G.; Wink, D. A.; Roberts, D. D. Nitric oxide in wound- healing. *Microsurgery* **2005**, *25*, 442–451.

(10) Schaffer, M. R.; Tantry, U.; Efron, P. A.; Ahrendt, G. M.; Thornton, F. J.; Barbul, A. Diabetes-impaired healing and reduced wound nitric oxide synthesis: a possible pathophysiologic correlation. *Surgery* **1997**, *121*, 513–519.

(11) Witte, M. B.; Kiyama, T.; Barbul, A. Nitric oxide enhances experimental wound healing in diabetes. *Br. J. Surg.* **2002**, *89*, 1594–1601.

(12) Ignarro, L. J. Biosynthesis and metabolism of endothelium-derived nitric oxide. *Annu. Rev. Pharmacol. Toxicol.* **1990**, *30*, 535–560.

(13) Wang, P. G.; Cai, T. B. *Nitric Oxide Donors*; Taniguchi, N., Eds.; Wiley-VCH: Weinheim, 2005.

(14) Wang, P. G.; Xian, M.; Tang, X.; Wu, X.; Wen, Z.; Cai, T.; Janczuk, A. J. Nitric oxide donors: chemical activities and biological applications. *Chem. Rev.* **2002**, *102*, 1091–1134.

(15) Napoli, C.; Ignarro, L. J. Nitric oxide-releasing drugs. *Annu. Rev. Pharmacol. Toxicol.* **2003**, *43*, 97–123.

(16) Miller, M. R.; Megson, I. L. Recent development in nitric oxide donor drugs. *Br. J. Pharmacol.* **2008**, *151*, 305–321.

(17) Smith, D. J.; Chakravarthy, D.; Pulfer, S.; Simmons, M. L.; Hrabie, J. A.; Citro, M. L.; Saavedra, J. E.; Davies, K. M.; Hutsell, T. C.; Mooradian, D. L.; Hanson, S. R.; Keefer, L. K. Nitric oxide-releasing polymers containing the [N(O)NO]- group. *J. Med. Chem.* **1996**, *39*, 1148–1156.

(18) Batchelor, M. M.; Reoma, S. L.; Fleser, P. S.; Nuthakki, V. K.; Callahan, R. E.; Shanley, C. J.; Politis, J. K.; Elmore, J.; Merz, S. I.; Meyerhoff, M. E. More lipophilic dialkyldiamine-based diazeniumdiolates: synthesis, characterization, and application in preparing thromboresistant nitric oxide release polymeric coatings. *J. Med. Chem.* **2003**, *46*, 5153–5161.

(19) Zhou, Z.; Meyerhoff, M. E. Preparation and characterization of polymeric coatings with combined nitric oxide release and immobilized active heparin. *Biomaterials* **2005**, *26*, 6506–6517.

(20) Kröncke, K. D.; Suschek, C. V. Adulterated effect of nitric oxide-generating donors. *J. Invest. Dermatol.* **2008**, *128*, 258–260.

(21) Bauer, J. A.; Rao, W.; Smith, D. J. Evaluation of linear polyethyleneimine/nitric oxide adduct on wound repair: therapy versus toxicity. *Wound Rep. Reg.* **1998**, *6*, 569–577.

(22) Arnold, E. V.; Doletski, B. G.; Raulli, R. E. Nitric oxide-releasing molecules. International Patent Application No. PCT/US05/000174.

(23) http://home.ncifcrf.gov/lcc/nitricoxide/NOdonors.asp.

(24) http://www.amuletpharma.com/techplatforms.html.

(25) Richardson, G.; Benjamin, N. Potential therapeutic uses for S-nitrosothiols. *Clin. Sci.* **2002**, *102*, 99–105.

(26) Williams, D. L. H. The mechanism of nitric oxide formation from S-nitrosothiols (thionitrites). *Chem. Commun.* **1996**, *10*, 1085–1091.

(27) Roy, B.; dïHardemare, A. D.; Fontecave, M. New thionitrites: synthesis, stability, and nitric oxide generation. *J. Org. Chem.* **1994**, *59*, 7019–7026.

(28) Lu, D.; Nadas, J.; Zhang, G.; Johnson, W.; Zweier, J. L.; Cardounel, A. J.; Villamena, F. A.; Wang, P. G. 4-Aryl-1,3,2-oxathiazolylium-5-olates as pH-controlled NO-donors: the next generation of S-nitrosothiols. *J. Am. Chem. Soc.* **2007**, *129*, 5503–5514.

(29) Katsumi, H.; Nishikawa, M.; Ma, S. F.; Yamashita, F.; Hashida, M. Physicochemical, tissue distribution, and vasodilation characteristics of nitrosated serum albumin: delivery of nitric oxide *in vivo*. *J. Pharm. Sci.* **2004**, *93*, 2343–2352.

Alternatively, synthetic polymers physically blended with RSNO have also been evaluated as NO delivery vehicles. In this regard, de Oliveira and co-workers incorporated NO donors such as GSNO and/or *S*-nitroso-*N*-acetylcysteine (SNAC) into films and gels based on water-soluble polymers such as poly(vinyl alcohol), poly(vinyl pyrrolidone), or Pluoronic F127 hydrogel, and evaluated such physical blends for topical NO delivery.[31−33] Their animal results suggest that daily repeated application of GSNO-blended hydrogels during the early phases of cutaneous wound repair may accelerate wound closure and re-epithelialization.[34] However, these physically blended NO donor systems still inherit the same drawbacks of free RSNOs such as rapid NO release and inactivation upon contact with physiological fluids due to thermal or metal ion catalyzed degradation. As a result, the delivery of NO from these existing RSNO based systems cannot be maintained for any extended duration, generally not more than several hours, thus requiring frequent reapplication from freshly prepared systems.

In order to achieve a meaningful extension of NO release duration, the macromolecular prodrug approach with *S*-nitrosothiol groups covalently attached to the polymer backbone appears to be a viable strategy for enhancing the stability of RSNOs, as well as in controlling the release duration of NO. In this regard, Bohl and West synthesized *S*-nitrosocysteine (CysNO)-derived PEG-hydrogels which exhibited reduced platelet adhesion and smooth muscle cell proliferation in cell culture.[35] Despite this seemingly encouraging result, most of the NO release occurred in the first 4 h and the achievable level of NO loading in these hydrogels remained very low (<1% w/w, based on stoichiometric data). On the other hand, de Oliveira and co-workers synthesized hydrophobic sulfhydryl (−SH)-containing polyesters followed by S-nitrosation in a gaseous NO/O_2 mixture.[36] The resulting hydrophobic polymeric NO donors provided localized NO release and showed enhanced local vasodilation when applied to the skin. Although such covalent anchoring of SNO groups has provided some degree of sustained release of NO, the achievable release duration remained relatively short (up to only 24 h). In addition, the complexities of their synthesis and the unknown toxicity of many of the building blocks and degradation products make it more difficult for these proposed polymeric NO donors to gain quick clinical utility. Therefore, there remains a need for a facile preparation of stable, *S*-nitrosothiol derived polymeric NO donors based on biocompatible and pharmaceutically acceptable components, capable of achieving effective loading and durable release of NO, suitable for a variety of clinical applications.

In this study, we report the synthesis of new phytochelatin-derived NO precursors (*S*-nitrosophytochelatins or *S*-nitrosoPCs) and the subsequent formation for the first time of a novel series of polymeric NO donors based on interpolymer complexes containing immobilized RSNOs (GSNO and *S*-nitrosoPCs) stabilized in a physically cross-linked polymer network. More specifically, RSNO precursors covalently conjugated to a maleic anhydride copolymer, poly(vinyl methyl ether-*co*-maleic anhydride) (PVMMA), are further stabilized in a physically cross-linked polymer network through intermolecular hydrogen bonding with poly(vinyl pyrrolidone) (PVP) in the solid state. Here, the existence of noncovalent interactions such as hydrogen bonding plays an important role in the self-assembly and formation of interpolymer complexes in solution as well as in the solid state.[37] Similar to the structure of glutathione (GSH) (Scheme 1A), phytochelatins (PCs) (Scheme 1B) are a family of oligomeric derivatives of GSH having the primary structure of $(\gamma\text{-Glu-Cys})_n\text{-Gly}$, where $n = 2-11$, produced by plants to chelate excess metal ions.[38] Recently, these plant derived peptides have been utilized as biocompatible coatings to modulate the surface properties of CdSe/ZnS nanocrystals.[39] The interpolymer complexes obtained in the present study are capable of providing continuous and prolonged NO generation with enhanced RSNO storage stability. Furthermore, all components of the present system are either endogenous in origin (e.g., GSH and GSNO) or biocompatible (e.g., PCs), or have prior history of use in humans as well as in approved drug products (e.g., PVMMA and PVP). In addition to

(30) Katsumi, H.; Nishikawa, M.; Yamashita, F.; Hashida, M. Development of polyethylene glycol-conjugated poly-*S*-nitrosated serum albumin, a novel *S*-nitrosothiol for prolonged delivery of nitric oxide in the blood circulation *in vivo*. *J. Pharmacol. Exp. Ther.* **2005**, *314*, 1117–1124.

(31) Seabra, A. B.; Da Rocha, L. L.; Eberlin, M. N.; de Oliveira, M. G. Solid films of blended poly(vinyl alcohol)/poly(vinyl pyrrolidone) for topical S-nitrosoglutathione and nitric oxide release. *J. Pharm. Sci.* **2005**, *94*, 994–1003.

(32) Shishido, S. M.; Seabra, A. B.; Loh, W.; de Oliveira, M. G. Thermal and photochemical nitric oxide release from S-nitrosothiols incorporated in Pluronic F127 gel: potential uses for local and controlled nitric oxide release. *Biomaterials* **2003**, *24*, 3543–3553.

(33) Seabra, A. B.; Fitzpatrick, A.; Paul, J.; de Oliveira, M. G.; Weller, R. Topically applied S-nitrosothiol-containing hydrogels as experimental and pharmacological nitric oxide donors in human skin. *Br. J. Dermatol.* **2004**, *151*, 977–983.

(34) Amadeu, T. P.; Seabra, A. B.; de Oliveira, M. G.; Costa, A. M. A. S-Nitrosoglutathione-containing hydrogel accelerates rat cutaneous wound repair. *J. Eur. Acad. Dermatol. Venereol.* **2007**, *21*, 629–637.

(35) Bohl, K. S.; West, J. L. N itric oxide-generating polymers reduce platelet adhesion and smooth muscle cell proliferation. *Biomaterials* **2000**, *21*, 2273–2278.

(36) Seabra, A. B.; da Silva, R.; de Oliveira, M. G. Polynitrosated polyesters: preparation, characterization, and potential use for topical nitric oxide release. *Biomacromolecules* **2005**, *6*, 2512–2520.

(37) Jiang, M.; Li, M.; Xiang, M.; Zhou, H. Interpolymer complexation and miscibility enhancement by hydrogen bonding. *Adv. Polym. Sci.* **1999**, *146*, 121–196.

(38) Rauser, W. E. Phytochelatins and related peptides: structure, biosynthesis, and function. *Plant Physiol.* **1995**, *109*, 1141–1149.

(39) Pinaud, F.; King, D.; Moore, H. P.; Weiss, S. Bioactivation and cell targeting of semiconductor CdSe/ZnS nanocrystals with phytochelatin-related peptides. *J. Am. Chem. Soc.* **2004**, *126*, 6115–6123.

Scheme 1. Chemical Structure of (A) Glutathione (GSH) and (B) Phytochelatin

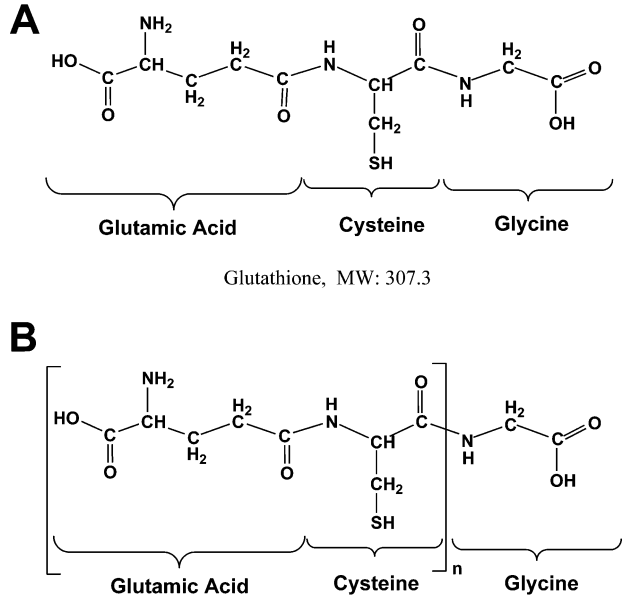

presenting the preparation and characterization of these novel RSNO−PVMMA/PVP interpolymer complexes, we also report the use of a diabetic rat model to assess the benefit of one such polymeric NO delivery system in wound healing.

Materials and Methods

Materials. Reduced glutathione (GSH), sodium nitrite ($NaNO_2$), sulfanilamide (SULF) and *N*-(1-naphthyl)ethylenediamine dihydrochloride (NEDD) were obtained from Sigma-Aldrich Canada (Oakville, ON). Phytochelatins, $(\gamma$-Glu-Cys$)_n$-Gly, with $n = 2$ and 5 (PC2 and PC5, respectively) were purchased from AnaSpec Inc. (San Jose, CA). Poly(vinyl methyl ether-*co*-maleic anhydride) (PVMMA, Gantrez AN-169, MW: 2,000,000) and poly(vinyl pyrrolidone) (PVP Plasdone K-90, MW: 1,300,000) were generously provided by ISP (Wayne, NJ). Other chemicals and solvents of analytical reagent grade were obtained from Sigma-Aldrich Canada, and they were used as received unless stated otherwise. Milli-Q grade (Millipore; Billerica, MA) deionized water was used for all solutions and buffers.

Synthesis of RSNOs. GSNO was readily prepared by reacting GSH with equimolar sodium nitrite in an acidic medium protected from exposure to light. Briefly, to a stirred ice-cold solution of GSH (154 mg, 0.5 mmol) in 5 mL of 0.1 N HCl was added a portion of $NaNO_2$ (35 mg, 0.5 mmol). This reaction gave GSNO in a high yield of more than 80% (equivalent to the fractional conversion of $NaNO_2$ determined by the Griess Assay as described in the section below on *in vitro* NO release). The resulting GSNO stock solution (red color) was protected from light with aluminum foil and used directly without further purification.

The S-nitrosation of phytochelatins (PC2 and PC5) was carried out in a similar fashion as GSNO, except that the molar ratio of PC2 and PC5 to $NaNO_2$ was 1:2 and 1:5 to account for the increasing number of thiol groups on PC2 and PC5, respectively.

Conjugation of RSNOs to PVMMA. The facile attachment of RSNOs to PVMMA was achieved via a heterogeneous reaction of RSNO with PVMMA. In the case of GSNO, 500 mg of PVMMA was first dissolved homogeneously in 10 mL of acetone. The above GSNO stock solution (2 mL) was then added dropwise into the PVMMA solution under stirring in an ice bath. Subsequently, the mixture was poured onto a Teflon dish and acetone was removed by either vacuum drying or air-drying in a fume hood at room temperature and protected from light. The obtained GSNO−PVMMA in the form of pink powder with 11.86 wt % GSNO loading was collected and stored in a desiccator. Additionally, a portion of the resultant solution was kept without drying and protected from light until the next complexation step. The conjugation of *S*-nitrosoPC2 and *S*-nitrosoPC5 to PVMMA was achieved in an identical fashion.

Preparation of RSNO−PVMMA/PVP Interpolymer Complexes. For RSNO−PVMMA/PVP complexes, a 6.36 wt % PVP solution was first prepared in a mixture of 10:1 (v/v) acetone and ethanol. In the case of GSNO−PVMMA, 4 mL of ethanol was added to the GSNO−PVMMA solution (in 10/2 acetone/0.1 N HCl) prior to the complex formation. Subsequently, a measured amount of the PVP solution was quickly poured into the GSNO−PVMMA solution under vigorous stirring in an ice bath. As the complex formation took place through intermolecular hydrogen bonding, the viscosity of the resultant mixture increased significantly giving rise to a pink gel-like product with the extent of gelation varying with composition. Although the PVMMA/PVP weight ratio can be varied by adjusting the volume of PVP solution, only 1:1 ratio was selected as an example for this study. The polymer complex so obtained, with 6.3 wt % GSNO loading, was air-dried, mixed with dry ice and pulverized in a laboratory grinding mill. The resulting pink powder was stored in amber glass vials prior to subsequent *in vitro* characterization and animal studies. Likewise, *S*-nitrosoPC2−PVMMA/PVP (1:1) and *S*-nitrosoPC5−PVMMA/PVP (1:1) were also prepared following identical procedures.

UV−Vis Spectra. The presence of the S−NO group in both RSNO and RSNO-conjugated PVMMA/PVP complex was verified via the appearance of characteristic absorbance maxima at 336 and 545 nm in the UV and visible ranges corresponding to $\pi \rightarrow \pi^*$and $n_N \rightarrow \pi^*$electronic transition of the S−NO bond, respectively.[32,36] UV−vis spectra were recorded in the wavelength range of 200−800 nm at room temperature on a Cary 50 UV−vis spectrophotometer (Varian Inc., Palo Alto, CA).

FTIR Spectra. The attachment of GSNO to PVMMA and hydrogen bonding interaction between GSNO−PVMMA and PVP were characterized by Fourier transform infrared (FTIR) on a universal attenuated total reflectance (ATR) Spectrum-one Perkin-Elmer spectrophotometer (Perkin-Elmer, Walth-

am, MA). The spectra were recorded from 650 to 4000 cm^{-1}. All spectra were collected at a resolution of 2 cm^{-1} and were repeated three times. A background spectrum without any sample was subtracted from all spectra.

Raman Spectra. Raman spectra were acquired using a Raman spectroscopy system (LabRam HR800, Jobin Yvon, France), which is equipped with a liquid-nitrogen-cooled CCD and a confocal microscope system (Olympus, BX41) with 3 objectives and a 60× (NA 0.9) water objective. The 325 nm line of a He−Cd UV-laser (Kimmon IK3301R-G) with a spot size of 1 μm was used as the excitation source. Samples of GSNO−PVMMA/PVP (1:1) lyophilized powder, before and after 24 h NO release, were evenly spread on individual microscope slides. Raman spectra were recorded at room temperature in the spectral region from 200 to 1200 cm^{-1} covering the S-S and C-S vibrational modes.

***In Vitro* NO Release.** The *in vitro* release study was typically carried out in a scintillation vial by immersing 20 mg of powder sample in 10 mL of 0.1 M phosphate buffered saline (PBS; pH 7.4) containing 0.1 wt % Na_2EDTA for the duration of the release experiment. The addition of chelating agent Na_2EDTA was to minimize any degradation of RSNO in the release medium catalyzed by metal ions. Multiple sample vials were placed on a vial rotator at a rotating speed of 15 rpm maintained at either room temperature (22 °C) or 37 °C in an incubator under a selected lighting condition. For continuous light exposure, the samples were exposed to fluorescent lamps (two USHIO F25T8/741 fluorescent tubes; 4100K) at an intensity of approximately 500 lx at the vial surface (measured with a light meter). These fluorescent lamps exhibit a spectral power distribution between 400 and 750 nm with about 55% of the total power output in the range of 530−620 nm.[40] The visible spectral range of 550−600 nm has been reported to be responsible for a major portion of the photoinitiated NO release from *S*-nitrosothiols.[41] For ambient light conditions, the samples were exposed to a normal day/night cycle in the laboratory with no special lighting control. To obtain cumulative NO release, the measurement was performed by consuming individual samples at predetermined time intervals. The release medium of each vial was then sampled and the NO release from the polymer immediately quantified by the standard Griess assay. Briefly, 1 mL of Griess reagent (NEDD) (0.1% w/v) plus 1 mL of sulfanilamide (1% w/v in 5% w/v H_3PO_4) at room temperature was incubated with an equal volume (1 mL) of the release medium. UV-vis absorbance of the resulting solution was determined at 540 nm, and the total nitrite concentration [NO_2^-] in the sample solution was calculated from a standard curve and converted to cumulative NO release expressed as nmol/mg of sample. Each datum point in the resulting NO release profile represents the mean of triplicate samples ($n = 3$) with the error bar denoting the standard deviation. The determination of nitrite, a stable decomposition product of NO, in solution using the Griess assay to provide a quantitative measure of NO release from various NO donors has been widely accepted.[35,36,42,43]

Decomposition Kinetics in Release Medium. The decomposition kinetics of GSNO−PVMMA/PVP complex versus that of GSNO in the release medium was studied employing the same experimental setup, temperature and light conditions as described in the previous section for the *in vitro* NO release. At time zero, either a GSNO−PVMMA/PVP complex powder sample or a small aliquot of the GSNO stock solution having identical GSNO content was mixed with the release medium and protected from light. After 2 days in the dark, the sample vials were switched to continuous light exposure for the remainder of the experiment. Throughout the entire duration of the experiment, the release medium was sampled at predetermined time intervals for a rapid determination of GSNO concentration by the UV method. These samples of the release medium were protected from light before and after the UV reading, and immediately returned to the sample vials for the continuation of the studies. The change in GSNO concentration in the release medium due to cleavage of S−N bond from exposure to different lighting and temperatures conditions was monitored by following the decay of UV absorbance at 336 nm as a function of time. This method is specific to changes in the GSNO concentration and not affected by the degradation products of NO as the UV absorbance of nitrite and nitrate is negligibly small between 300 and 400 nm in the μmol concentration range studied here.

Stability Studies. In one experiment, GSNO−PVMMA/PVP (1:1) complex powder was stored in glass vials at room temperature (relative humidity: ~32%.) without protection from light for a duration of 6 months. In another experiment, GSNO−PVMMA/PVP (1:1) complex powder was exposed to direct UV irradiation from a UV lamp in a Labguard Class II Biological Safety Cabinet (66 cm height, 15 W UV light) for 24 h. The NO release profiles from these stability samples were determined and compared with that of the original samples.

Additionally, the stability of GSNO, *S*-nitrosoPC5 and *S*-nitrosoPC5−PVMMA/PVP (1:1) complex in PBS in the presence of copper ion was investigated by monitoring the decay of UV absorbance at 336 nm in sample solutions containing a fixed concentration of Cu^{2+} (36 μM).

***In Vivo* Wound Healing.** The animal study was performed under an animal protocol approved by the University of Toronto Animal Care Committee. Briefly, 15 male Sprague−

(40) http://www.ushio.com/files/specs/Ultra8T8UBend.pdf.
(41) Frost, M. C.; Meyerhoff, M. E. Controlled photoinitiated release of nitric oxide from polymer films containing *S*-nitroso-*N*-acetyl-DL-penicillamine derivatized fumed silica filler. *J. Am. Chem. Soc.* **2004**, *126*, 1348–1349.
(42) Mowery, K. A.; Schoenfisch, M. H.; Saavedra, J. E.; Keefer, L. K.; Meyerhoff, M. E. Preparation and characterization of hydrophobic polymeric films that are thromboresistant via nitric oxide release. *Biomaterials* **2000**, *21*, 9–21.
(43) Nims, R.; Cook, J.; Krishna, M.; Christodoulou, D.; Poore, C.; Miles, A.; Grisham, M.; Wink, D. Colorimetric assays for nitric oxide and nitrogen oxide species formed from nitric oxide stock solutions and donor compounds. *Methods Enzymol.* **1996**, *268*, 93–105.

Dawley rats (Charles River, Montreal, QC) were acclimatized for one week, given food and water ad libitum. Seven days before wounding, the animals were injected intraperitoneally (IP) with streptozotocin (60 mg per kg body weight in citrate buffer 0.1 mol/L, pH 4.5) to induce diabetes. Evidence of diabetes was confirmed by blood glucose levels greater than 14 mmol/L and frequent urination. Animals not achieving the diabetic state after 24 h were reinjected with streptozotocin. Subsequently, animals with blood glucose level still remaining below14 mmol/L were excluded from the study. After the induction of diabetics, the blood glucose level was monitored twice a week to ensure that the diabetic state was maintained throughout the entire wound healing experiment.

For the surgery, animals were weighed and assigned to two groups (5 for the control and 7 for the test group; three excluded). The following procedures were conducted while animals were anesthetized with isoflurane inhalation. First, the dorsal surface hair was removed by shaving and the skin washed with povidone−iodine solution and 70% alcohol. Subsequently, a full thickness excisional wound was created by removal of the skin and panniculus carnosus using an 8 mm biopsy punch. Rats were given analgesic (ketoprofen, 5 mg/kg, sc) immediately after surgery. At the wound sites, the control group was treated with 20 mg of blank PVMMA/PVP complex powder without GSNO loading, while the test group was treated with 20 mg of GSNO−PVMMA/PVP (1:1) complex powder (6.3 wt % GSNO loading). The GSNO loading level and the amount of complex powder were selected to ensure the delivery of μmol quantity of GSNO per application and the complete coverage of each wound area by the powder. All polymer powders quickly adhered to the wound tissue with the addition of two drops of sterile saline. After a single application of the polymer powder, wounds were covered with transparent Tagederm dressings (3M; St. Paul, MN) sealed at the edges with tincture of benzoin (Benzoin Simple Tincture NF; Xenex Laboratories, Ferndale, WA). Afterward, animals were transferred to individual cages and maintained on a standard diet, allowed access to water ad libitum. All animal experiments were conducted under ambient light conditions.

At selected time points during the postwounding period, the animals were anesthetized by isoflurane inhalation and photographs of the wound sites were recorded using a digital camera; a calibration scale was also recorded with each photograph. During the first 7 days after wounding, the Tegaderm dressing was changed daily. Beyond 7 days, the wounds were no longer covered with dressings. The surface area of each lesion was quantified from the photographs using Image-Pro Plus 5.0 software to determine the area of the open wound. The results are expressed in percentage of initial wound area as a function of time. For each datum point, mean and standard deviation were calculated. Statistical analysis between experimental groups was performed using unpaired two-tailed Student's *t* tests. The confidence limit was predetermined at an alpha level of 0.05.

Scheme 2. (A) Conjugation of RSNO to PVMMA and (B) Hydrogen Bonding Interaction between RSNO−PVMMA and PVP

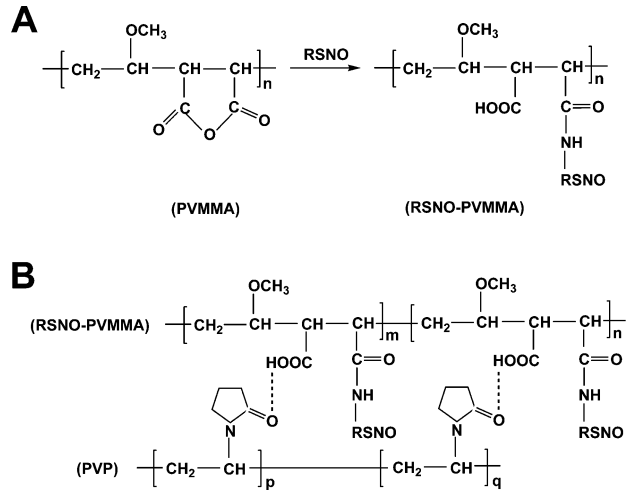

Results and Discussion

Synthesis and Characterization. GSNO, *S*-nitrosoPC2 and *S*-nitrosoPC5 were prepared via nitrosation of thiols according to the following reaction scheme:

$$\mathrm{RSH} + \mathrm{HNO_2} \xrightarrow{\mathrm{H_3O^+}} \mathrm{RSNO} + \mathrm{H_2O} \qquad (1)$$

This reaction is generally very rapid and quantitative. Although GSNO is a known NO precursor, phytochelatin-derived NO precursors synthesized here such as *S*-nitrosoPC2 and *S*-nitrosoPC5 are new. One key advantage of the present NO precursors over other systems is that GSH and phytochelatins are short, cysteine rich peptides, which can provide high levels of NO loading after nitrosation.[16,17]

Following the reaction scheme of Scheme 2A, *S*-nitrosoPC2 and *S*-nitrosoPC5 have been conjugated to PVMMA also for the first time to form a novel series of polymeric NO precursors. A notable characteristic of maleic anhydride copolymers such as PVMMA is the high reactivity between the anhydride moieties and primary amine groups. Covalent modification of proteins with maleic anhydride was reported as early as the 1960s;[44] such a reaction can be beneficially performed via surface chemistry following the interfacial presentation of bioactive molecules.[45,46] In our case, the conjugation of RSNO to PVMMA was achieved via a heterogeneous reaction because RSNO has to be dissolved

(44) Butler, P. J. G.; Harris, J. I.; Hartley, B. S.; Leberman, R. Use of maleic anhydride for reversible blocking of amino groups in polypeptide chains. *Biochem. J.* **1969**, *112*, 679–689.

(45) Ladavière, C.; Lorenzo, C.; Elaïssari, A.; Mandrand, B.; Delair, T. Electrostatically driven immobilization of peptides onto (maleic anhydride-*alt*-methyl vinyl ether) copolymers in aqueous media. *Bioconjugate Chem.* **2000**, *11*, 146–152.

(46) Allard, L.; Cheynet, V.; Oriol, G.; Mandrand, B.; Delair, T.; Mallet, F. Versatile method for production and controlled polymer-immobilization of biologically active recombinant proteins. *Biotechnol. Bioeng.* **2002**, *80*, 341–348.

in 0.1 N HCl whereas PVMMA is only soluble in acetone, and because acetone and aqueous HCl are precipitating agents for RSNO and PVMMA, respectively. Therefore, the grafting reaction takes place only at the interface of RSNO and PVMMA in solution. Depending on the volume ratio and concentration of the two components, the RSNO loading level can be varied. Comparing with other NO delivery systems,[16,17] the abundance of functional anyhydride groups on the backbone of PVMMA enables the attachment of RSNOs with grafting degree as high as 50% for GSNO.

The complexation of RSNO−PVMMA and PVP is based on interpolymeric hydrogen bonding interactions depicted in Scheme 2B. The formation of interpolymer complexes via hydrogen bonding between a proton-donating polymer such as poly(carboxylic acid) and a proton-accepting nonionic polymer such as PVP has been extensively investigated for pharmaceutical purposes.[47,48] This is typically accomplished by first dissolving each polymer component separately in a common solvent followed by mixing the component solutions. The resulting formation of interpolymer complexes is often manifested by an increase in solution viscosity or the precipitation of a separate gel phase. In our study, poly(vinyl pyrrolidone) (PVP), which contains a large number of pendant pyrrolidone carbonyl groups, is used as a proton-accepting polymer to complex with the hydrolyzed portion of PVMMA in RSNO−PVMMA, which acts as a proton-donating polymer. Since RSNO−PVMMA is formed in an acetone based solvent and PVP does not dissolve in pure acetone, a small amount of ethanol was introduced in the PVP solution to facilitate the complex formation. To ensure that phase separation does not result from solvent induced PVP precipitation, a comparable amount of ethanol was also incorporated into the RSNO−PVMMA solution before blending with the PVP solution.

The presence of S−NO group in both GSNO and GSNO-conjugated PVMMA is demonstrated via the appearances of the characteristic absorbance of S−NO bond at $\lambda = 336$ nm and $\lambda = 545$ nm (see Figure 1A,B), corresponding to the maximum absorption in the UV and visible ranges, respectively. These have been assigned to the $\pi \rightarrow \pi^*$ and $n_N \rightarrow \pi^*$ electronic transitions of the S−NO bond, respectively. Likewise, in Figure 1C, the presence of an absorbance peak at $\lambda = 336$ nm verifies the successful synthesis of *S*-nitrosoPC5. A similar absorbance spectrum was also observed with *S*-nitrosoPC2 (data not shown).

The IR spectra of GSNO, PVMMA, GSNO−PVMMA, and GSNO−PVMMA/PVP (1:1) complex are shown together in Figure 2. The small band at 1706 cm^{-1}, originated from acid dimers likely formed from a trace amount of carboxylic acid groups in the PVMMA raw material (curve c), has been replaced by the characteristic ester carbonyl band at 1724 cm^{-1} (curves d and e), which can be attributed to

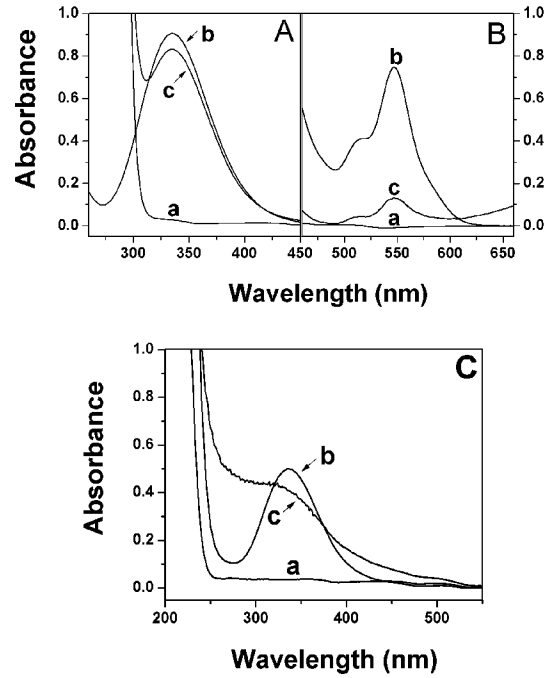

Figure 1. (A) UV and (B) visible spectra of (a) pure PVMMA in acetone, (b) GSNO in aqueous medium, and (c) GSNO−PVMMA in aqueous medium; and (C) UV−vis spectra of (a) pure PC5, (b) *S*-nitrosoPC5, and (c) *S*-nitrosoPC5−PVMMA/PVP (1/1) complex in aqueous medium.

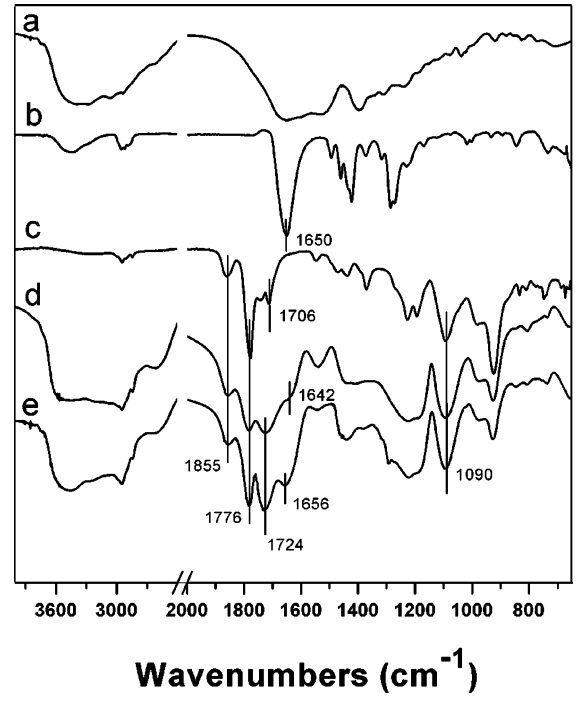

Figure 2. The FTIR spectra of (a) GSNO, (b) PVP, (c) PVMMA, (d) GSNO− PVMMA, and (e) GSNO−PVMMA/PVP (1/1) complex.

(47) Khutoryanskiy, V. V. Hydrogen-bonded interpolymer complexes as materials for pharmaceutical applications. *Int. J. Pharm.* **2007**, *334*, 15–26.

(48) Haddadine-rahmoun, N.; Amrani, F.; Arrighi, V.; Cowie, J. M. G. Interpolymer complexation in hydrolysed poly(styrene-co-maleic anhydride)/poly(styrene-co-4-vinylpyridine). *Eur. Polym. J.* **2008**, *44*, 821–831.

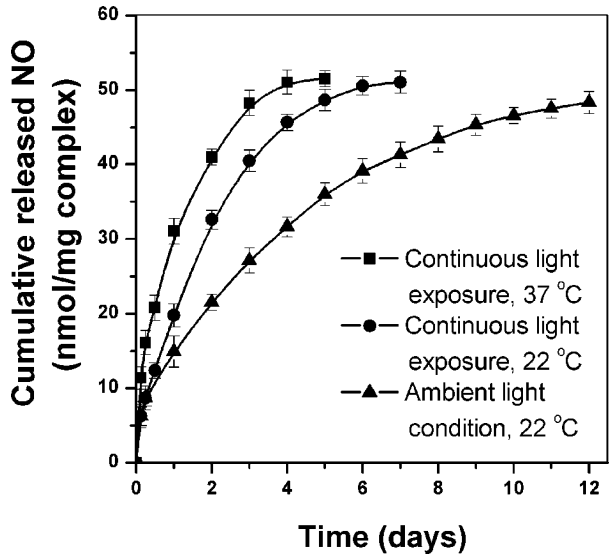

Figure 3. *In vitro* release profiles comparing NO release in 0.1 M phosphate buffer saline (containing 0.1 wt % Na_2EDTA) from GSNO−PVMMA/PVP (1/1) interpolymer complex powder containing 6.3 wt % of GSNO at 22 and 37 °C under different lighting conditions. Each datum point is the mean of three samples, and the error bar represents the standard deviation.

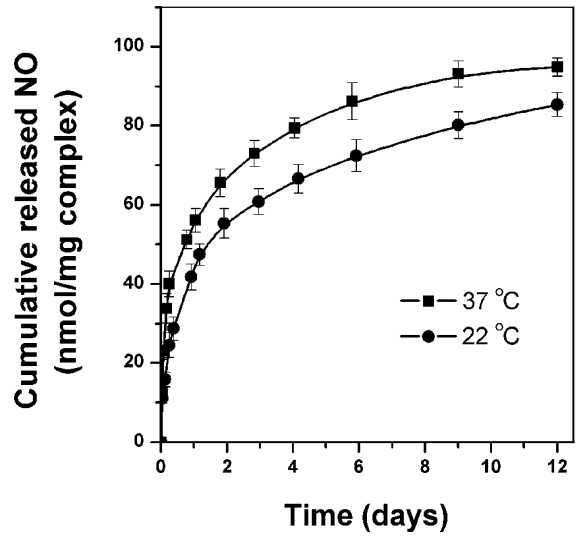

Figure 4. *In vitro* release profiles comparing NO release in 0.1 M phosphate buffer saline (containing 0.1 wt % Na_2EDTA) from *S*-nitrosoPC5−PVMMA/PVP (1/1) interpolymer complex powder containing 3.24 wt % of *S*-nitrosoPC5 at 22 and 37 °C under ambient light conditions. Each datum point is the mean of three samples, and the error bar represents the standard deviation.

their esterification with ethanol during the GSNO coupling process. Another major absorption band at 1642 cm^{-1} appears in the spectrum of GSNO-conjugated PVMMA (curve d) which is characteristic of the carbonyl group of an amide. This provides direct evidence for the acylation reaction between the anhydride group of PVMMA and the primary amino group of GSNO. The hydrogen bonding interaction in the present GSNO−PVMMA/PVP complex is also reflected in the IR spectra of Figure 2, where a shift of the carbonyl stretching band in the pyrrolidone ring from 1650 cm^{-1} in pure PVP (curve b) to 1656 cm^{-1} in the GSNO−PVMMA/PVP complex (curve e) is quite evident. Such an upward shift in carbonyl stretching frequency as a result of intermolecular hydrogen bonding is well-known in other miscible polymer blends.[49,50]

Effect of Temperature and Light on *in Vitro* NO Release. Typical profiles of NO release from the GSNO−PVMMA/PVP (1/1) complex (with 6.3 wt % GSNO loading) at 22 and 37 °C under continuous light exposure are shown in Figure 3, where the total amount of NO release is normalized to sample weight. For comparison, a corresponding NO release profile at 22 °C under ambient light conditions is also included in Figure 3. It is clear that the duration of NO release from the present interpolymer complex containing immobilized GSNO can be extended up to 10 days or more under ambient light conditions. In addition to the faster rate and shorter duration of NO release at elevated temperature (37 °C vs 22 °C), continuous light exposure also results in a faster NO release as compared with the ambient light condition where the exposure to light is of intermittent nature due to the natural day/night cycle. Nevertheless, as shown in Figure 3, even with faster NO release under continuous light exposure, the characteristic feature of sustained NO delivery from the present polymer complex is still retained with duration of release up to 7 days or more. The release profiles of Figure 3 represent about 40−50% of total NO release. Additional NO release is still possible with higher intensity of light irradiation. Further kinetic experiments relating to this aspect are currently ongoing.

Similarly, Figure 4 demonstrates the sustained NO release behavior from the *S*-nitrosoPC5−PVMMA/PVP (1:1) complex with 3.24 wt % *S*-nitrosoPC5 loading as a function of temperature under ambient light condition, where the release period is similarly extended up to at least 10 days and the release profiles represent about 60−70% of total NO release. Moreover, the use of PC5 as the NO donor enables a higher total amount of NO delivered per mg of sample due to the presence of more thiol groups on PC5. It is worth noting that *S*-nitrosoPC5−PVMMA/PVP (1:1) complexes exhibit solubility behavior that is quite different from that of GSNO−PVMMA/PVP (1:1). In our observations, *S*-nitroso-PC5−PVMMA/PVP (1:1) appeared to dissolve in phosphate buffer at room temperature, resulting in a gel-like solution within hours, whereas the dissociation of the GSNO−PVMMA/PVP (1:1) complex took several days. This aspect

(49) Lee, J. Y.; Painter, P. C.; Colman, M. M. Hydrogen bonding in polymer blends. 3. Blends involving polymers containing methacrylic acid and ether groups. *Macromolecules* **1988**, *21*, 346–354.

(50) Xu, X.; Lee, P. I. Programmable drug delivery from an erodible association polymer system. *Pharm. Res.* **1993**, *10*, 1144–1152.

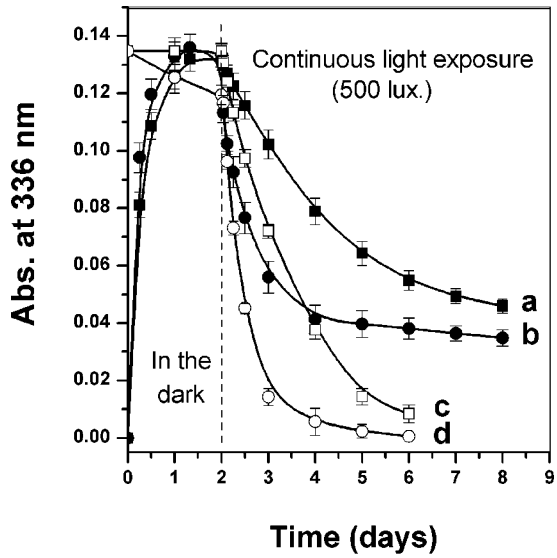

Figure 5. Decomposition kinetics of GSNO−PVMMA/PVP (1/1) interpolymer complex (a and b, 6.3 wt % of GSNO) versus that of free GSNO (c and d) in 0.1 M phosphate buffer saline (containing 0.1 wt % Na_2EDTA) at (a, c) 22 °C and (b, d) 37 °C; in the dark for the initial 2 days followed by continuous light exposure for 7 days. Each datum point is the mean of three samples, and the error bar represents the standard deviation.

is currently being further investigated to delineate the significance of such a difference in polymer erosion behavior.

Decomposition Kinetics in Release Medium. It is well-known that homolysis of RSNO forming disulfide bridges is the main mechanism responsible for its degradation which can be catalyzed by metal ions (e.g., Cu^{2+}), heat, and light:[51]

$$2\text{RSNO} \xrightarrow{\text{heat, light, and metal}} \text{RSSR} + 2\text{NO} \qquad (2)$$

Figure 5 illustrates the decomposition kinetics of GSNO−PVMMA/PVP (1:1) complex versus that of GSNO in the release medium at 22 and 37 °C under different lighting conditions, where the catalytic degradation of GSNO by metal ions has been minimized by the addition of Na_2EDTA, a chelating agent, in the release medium. A UV method rather than the Griess assay is employed here to allow for tracking the real time changes in GSNO concentration in the release medium from a single sample, whereas the Griess assay is more time-consuming and requires the consumption of one sample for each measurement. The UV absorbance reading correlates directly to the concentration of GSNO in the sample at any given time. It can be seen from curve c of Figure 5 that GSNO in PBS at pH 7.4 is quite stable at 22 °C when protected from light as there is no detectable decomposition during the initial 2 days. However, with the same initial GSNO concentration, curve d of Figure 5 shows some noticeable thermal decomposition at 37 °C in the dark after 2 days. On the other hand, curves a and b of Figure 5 show a gradual buildup of GSNO concentration over the same time period due to the erosion and slow dissolution of the GSNO−PVMMA/PVP (1:1) complex sample. In this case, the dissolution of the complex is complete at around 2 days at both 22 and 37 °C and there is a negligible loss of GSNO from the GSNO−PVMMA/PVP (1:1) complex in the release medium when protected from light for a period of 2 days as confirmed by independent Griess assays (data not shown). This suggests that the decomposition kinetics in the release medium in the dark appears to be less affected by temperature for the present GSNO−PVMMA/PVP (1:1) complex as compared with free GSNO.

The subsequent decomposition kinetics mediated by continuous light exposure and thermal effect is also shown in Figure 5. It is evident that the light-induced decomposition of GSNO can be significantly slowed by immobilizing GSNO in the present interpolymer complex (curves a and b) as compared with the rapid decomposition of free GSNO (curves c and d). For example, based on the absorbance data of Figure 5, around 40% of the conjugated GSNO groups still remain in the interpolymer complex after 6 days of continuous light exposure in the solution phase, whereas the free GSNO is almost depleted after only 4 days. On the other hand, the decomposition kinetics in the release medium under continuous light exposure seems to be similarly affected by temperature for both the GSNO−PVMMA/PVP (1:1) complex and free GSNO.

The decreased decomposition rate of GSNO−PVMMA/PVP (1:1) complex can be attributed to several factors. It is known that the NO release from GSNO and related compounds generally involves two steps,[51−53] one of which is due to homolytic bond cleavage via photoexcitation (eq 3); another involves subsequent reactions of the produced thiyl radical either directly with GSNO (eq 4) or with oxygen to produce the peroxy radical, which then reacts with GSNO to give GSSG (eqs 5 and 6).

$$\text{GSNO} \rightarrow \text{GS}\bullet + \text{NO}\bullet \qquad (3)$$

$$\text{GSNO} + \text{GS}\bullet \rightarrow \text{GSSG} + \text{NO}\bullet \qquad (4)$$

$$\text{GS}\bullet + \text{O}_2 \rightarrow \text{GSOO}\bullet \qquad (5)$$

$$\text{GSOO}\bullet + \text{GSNO} \rightarrow \text{GSSG} + \text{NO}\bullet + \text{O}_2 \qquad (6)$$

Similarly, upon NO generation in the case of the present GSNO−PVMMA/PVP (1:1) complex, macromolecular radi-

(51) Williams, D. L. H. The chemistry of S-nitrosothiols. *Acc. Chem. Res.* **1999**, *32*, 869–876.

(52) Sextona, D. L.; Ruganandadmo, R.; Mckenney, N. J.; Mutus, B. Visible light photochemical release of nitric oxide from *S*-nitrosoglutathione: Potential photochemotherapeutic applications. *Photochem. Photobiol.* **1994**, *59*, 463–461.

(53) Wood, P. D.; Mutus, B.; Redmond, R. W. The Mechanism of Photochemical Release of Nitric Oxide from S-Nitrosoglutathione. *Photochem. Photobiol.* **1996**, *64*, 518–524.

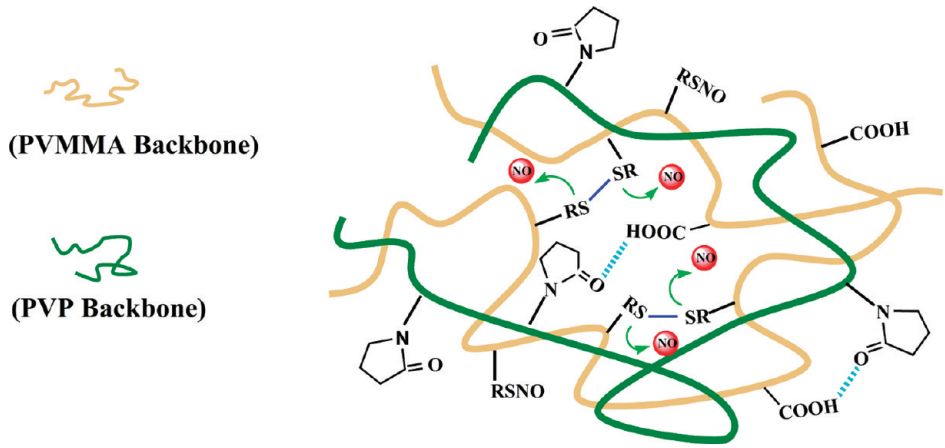

Figure 6. Molecular scheme depicting the NO release from the RSNO−PVMMA/PVP interpolymer complex network yielding disulfide bonds in the solid state.

cals PVMMA−GS• or PVMMA−GSOO• will form and recombine with GSNO−PVMMA, leading to the further liberation of NO and the formation of a dimer linked by the disulfide bridge. The increased bulkiness through chemical conjugation of GSNO with the macromolecule PVMMA leads to a slower diffusion rate (or reduced mobility) of the PVMMA−GS• or PVMMA−GSOO• radical as well as that of GSNO−PVMMA compared with the corresponding species derived from free GSNO. This results in a slower rate of recombination of these species and therefore a slower rate of NO release (or GSNO decomposition) from the current GSNO−PVMMA/PVP (1:1) complex as seen in Figure 5 (curves a and b). Therefore, compared with other reported RSNO-linked polymers,[36,54] the very high MW of PVMMA employed in the present study (MW 2,000,000) further reduces the rate of NO liberation and enhances the extent of the extended NO release observed here.

NO Release Mechanism. To gain additional insight into the mechanism of NO release from RSNO−PVMMA/PVP complexes, a proposed molecular scheme is depicted in Figure 6. It is envisioned that as the RSNO−PVMMA/PVP complex is in contact with an aqueous medium, the hydrophilic components of the polymer complex (hydrolyzed PVMMA and PVP) would swell, giving rise to increased polymer chain mobility, thus providing more opportunity for the pendant −SNO groups to come closer to each other. Although the rate of decomposition of RSNO (or rate of release of NO) is affected by heat, light, and metal ions as discussed above, the major rate limiting step seems to be the slower rate of diffusion (or reduced mobility) of the bulky PVMMA−GS• or PVMMA−GSOO• radical and its recombination with its parent molecule to release the NO and forming disulfide linkages as described in the previous section. As nitric oxide is gradually liberated from such a complex, more disulfide bonds will form giving rise to in situ disulfide cross-linking between RSNO side chains, which further reinforces the network structure of the complex. Such disulfide cross-linking would reduce the rate of erosion of the polymer complex in an aqueous medium, thereby preventing the polymeric complex from quickly dissolving in an aqueous medium and consequently further slowing the diffusion-limited process for the liberation of NO as reflected in the gradual leveling off of curves a and b of Figure 5 above, thus capable of prolonging the NO release at the local site of application. Depending on the polymer structure and state of chain packing, a different controlled release rate can be obtained by adjusting the RSNO loading, the component polymer molecular weight and the concentration ratio in the complex.

This proposed formation of disulfide bonds during NO release is verified by comparing the Raman spectra of the GSNO−PVMMA/PVP complex before and after NO release in Figure 7. The appearance of distinct Raman lines peaking at 455 cm^{-1} (S−S stretching) and 630 cm^{-1} (C−S stretching) is indicative of the formation of −CSSC−, confirming that some S−NO groups have been converted to disulfide bonds, thereby liberating NO. Although −SS− has also been associated with Raman bands excited at 514.5 nm radiation,[55,56] the selection of UV excitation at 325 nm in our Raman study is more convenient because it avoids the typical fluorescence background found in samples excited in the visible range.

Stability in the Presence of Copper Ion. Since copper can directly and catalytically trigger the decomposition of RSNO in solution,[57] the stability of GSNO, *S*-nitrosoPC5, and *S*-nitrosoPC5 conjugated PVMMA/PVP complex in the

(54) Stasko, N. A.; Fischer, T. H.; Schoenfisch, M. H. S-Nitrosothiol-modified dendrimers as nitric oxide delivery vehicles. *Biomacromolecules* **2008**, *9*, 834–841.

(55) Picquart, M.; Grajcar, L.; Baron, M. H.; Abedinzadeh, Z. Vibrational spectroscopic study of glutathione complexation in aqueous solutions. *Biospectroscopy* **1999**, *5*, 328–337.

(56) Brandt, N. N.; Chikishev, A. Y.; Kargovsky, A. V.; Nazarov, M. M.; Parashchuk, O. D.; Sapozhnikov, D. A.; Smirnova, I. N.; Shkurinov, A. P.; Sumbatyan, N. V. Terahertz time-domain and raman spectroscopy of the sulfur-containing peptide dimers: low-frequency markers of disulfide bridges. *Vib. Spectrosc.* **2008**, *47*, 53–58.

(57) Grossi, L.; Montevecchi, P. C. A kinetic study of S-nitrosothiol decomposition. *Chem. Eur. J.* **2002**, *8*, 380–387.

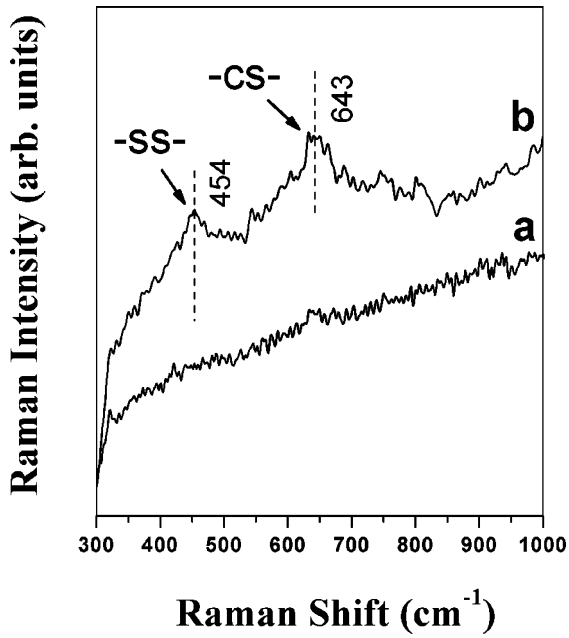

Figure 7. Comparison of Raman spectra of GSNO−PVMMA/PVP (1/1) complex (a) before and (b) after NO release.

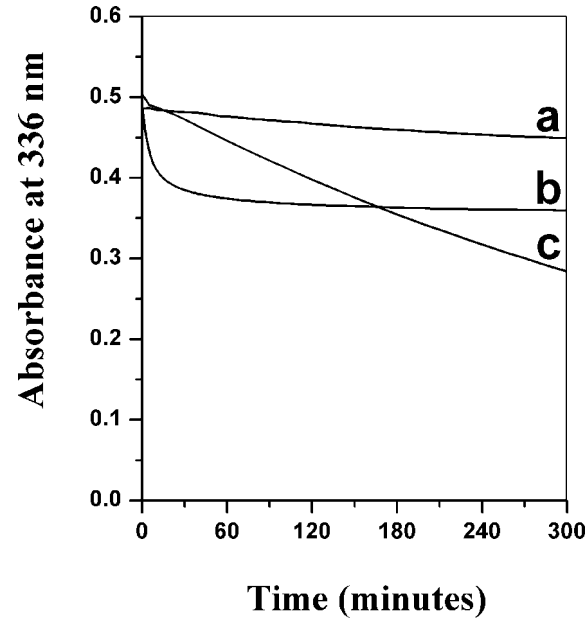

Figure 8. Decomposition kinetics of (a) *S*-nitrosoPC5−PVMMA/PVP (1/1) complex, (b) GSNO, and (c) *S*-nitrosoPC5 in the presence of 36 μM [Cu^{2+}] in 0.1 M PBS (pH 7.4).

presence of $CuSO_4$ in an aqueous solution has been evaluated and compared. The rate-determining step in this metal ion catalyzed decomposition process is known to be the reaction between RSNO and Cu^+ (eq 8), where Cu^+ can be generated by the thiolate reduction of Cu^{2+} (eq 7) and has been deemed to be the true catalyst.[51,58]

$$2RS^- + 2Cu^{2+} \rightarrow RSSR + 2Cu^+ \quad (7)$$

$$RSNO + Cu^+ \rightarrow RS^- + Cu^{2+} + NO \quad (8)$$

The stability data of GSNO, *S*-nitrosoPC5 and *S*-nitrosoPC5−PVMMA/PVP complex (with 3.24 wt % *S*-nitrosoPC5 loading) in phosphate buffer in the presence of copper ions are shown in Figure 8. It can be seen that GSNO exhibits a rapid degradation during the initial 20 min followed by a progressively halted decomposition (curve b in Figure 8). This seemingly incomplete degradation of GSNO through the copper ion pathway can be attributed to the known chelation reaction of Cu^{2+} with the GSSG already formed in solution,[59] which leads to less Cu^{2+} being available for reduction. It is believed that the disulfide bridges pull together the glutamate residues, facilitating the coordination of Cu^{2+} with sulfur or nitrogen atoms.[51]

In contrast to GSNO, *S*-nitrosoPC5 shows linear decomposition kinetics in the presence of copper from the same starting concentration of −SNO (curve c in Figure 8). This may be attributed to different complexation modes, as well as different Cu^{2+}:RSSR stoichiometries involving *S*-nitrosoPC5.

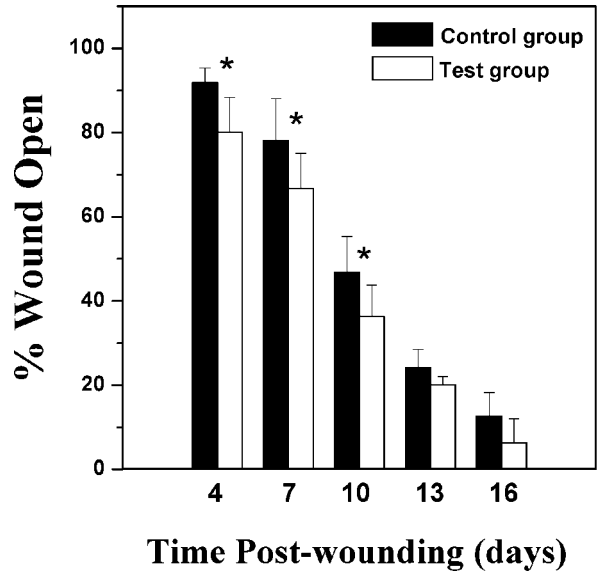

Figure 9. Macroscopic evaluation of wound closure in diabetic rats in GSNO−PVMMA/PVP (1/1) complex treated group ($n = 7$) versus the control group ($n = 5$), where * indicates $p < 0.05$.

On the other hand, *S*-nitrosoPC5−PVMMA/PVP shows a substantially enhanced stability over the other RSNOs (curve a in Figure 8); degradation of the complex is negligibly slow under the same reaction conditions during the initial 300 min. This is most likely due to the chelating

(58) Noble, D. R.; Williams, D. L. H. Structure-reactivity studies of the Cu^{2+}-catalyzed decomposition of four *S*-nitrosothiols based around the S-nitrosocysteine/S-nitrosoglutathione structures. *Nitric Oxide* **2000**, *4*, 392–398.

(59) Hogg, N. Biological chemistry and clinical potential of S-nitrosothiols. *Free Radical Biol. Med.* **2000**, *28*, 1478–1486.

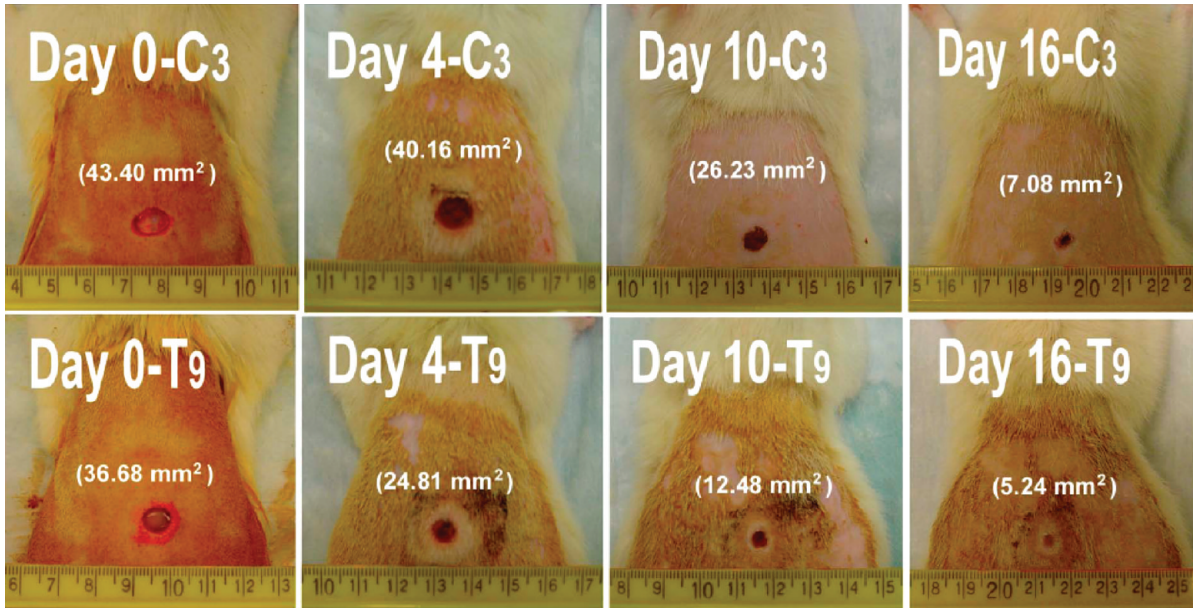

Figure 10. Representative photographs showing progression of wound healing in diabetic rats in GSNO−PVMMA/PVP (1/1) complex treated group (T_9) versus the control group (C_3) at days 0, 4, 10, and 16 after wounding. The ruler scale is 8 cm in all images. The integrated wound area is indicated in each photograph.

effect of the carboxylic acid polymer derived from hydrolysis of the polyanhydride component (PVMMA) in the buffer. This way, most of the Cu^{2+} may be removed from the solution and not available to catalyze the decomposition, thus resulting in enhanced stability.

Stability in the Solid State. As described above, the conjugation of RSNO to PVMMA increases the bulkiness of RSNO. Additionally, the physical interaction of PVMMA and PVP in the complex effectively limits the mobility of RSNO. Thus, the restricted mobility of macromolecular radicals (PVMMA−GS•), due in part to the glassiness of the physically cross-linked network in the solid state, is expected to reduce the rate of decomposition by the collision process. As a result, the present complex system remarkably enhances the stability of RSNO in the solid state. There is no significant change in the NO release profile after 6 months storage or prolonged exposure to UV irradiation of the GSNO−PVMMA/PVP complex powder under ambient conditions (data not shown). This is indicative of the stability of the present complex system in the solid state when stored under room conditions.

Animal Studies. Wound closure data based on a diabetic rat model are plotted in Figure 9, which demonstrate that topical application of the present NO-releasing GSNO−PVMMA/PVP (1:1) complex system can effectively accelerate wound closure. There is a statistically significant difference in wound closure tendency between the control and test group ($p < 0.05$) on days 4, 7 and 10, whereas the difference becomes less significant on days 13 and 16. This may be related to the fact that the NO release from the present complex generally lasts only up to 10 days or so (see Figure 3). Representative photographs of full thickness wounds showing the progression of wound healing in the test group versus the control on days 0, 4, 10, and 16 are presented in Figure 10. The apparent overall wound condition in terms of wound closure and healing also appears to be better in the test group than in the control group on days 4, 10, and 16 after wounding. These preliminary results strongly suggest that the present controlled release NO delivery systems based on GSNO−PVMMA/PVP interpolymer complexes could be potentially useful in enhancing wound healing.

Conclusions

In conclusion, we have developed a novel but stable and biocompatible platform for generating a durable release of NO. We have reported the facile synthesis of new phytochelatin-derived NO precursors (*S*-nitrosophytochelatins or *S*-nitrosoPCs) and the formation for the first time of a novel series of polymeric NO donors based on interpolymer complexes between RSNO (GSNO and *S*-nitrosoPCs) conjugated PVMMA and poly(vinyl pyrrolidone) (PVP) through intermolecular hydrogen bonding. In this case, the immobilized NO precursors (RSNOs) are further stabilized in a physically cross-linked polymer network. As a result, the present interpolymer complex system exhibits remarkable stability enhancement of immobilized GSNO in the solid state as well as in the release medium due to significantly reduced mobility of the resulting macromolecular glutathione radicals leading to reduced rate of decomposition compared with that of the free GSNO. In addition, the present complex system also exhibits a substantial enhancement of stability in the presence of copper ion in the release medium. The existence of intermolecular hydrogen bonding in the present

system and the formation of disulfide bonds as a result of the NO release have been confirmed by FTIR and Raman spectroscopy, respectively. We have also shown that the present system is capable of providing sustained and controlled release of NO for an extended duration of up to 10 days or more. Preliminary *in vivo* testing in a diabetic rat model demonstrates that topical application of the present controlled release NO delivery system can effectively accelerate wound closure. There is a statistically significant difference in wound closure tendency between the control and test group during NO release ($p < 0.05$). Since all functional components of the present system have had prior history of use in humans as well as in approved drug products, this novel nitric oxide releasing platform can be readily incorporated into dressings, patches and bandages for diabetic wound treatment. Further studies to determine the range of NO delivery rate suitable for diabetic wound healing and to demonstrate enhanced wound healing quality through histological assessment are in progress.

Acknowledgment. This work was supported by funding from the Natural Sciences and Engineering Research Council of Canada (NSERC).

MP900237F